Journal of Applied Polymer Science

Hybrid biocomposites with enhanced thermal and mechanical properties for structural applications

K. C. Birat,[1] Suhara Panthapulakkal,[1] Andrei Kronka,[2] Jose Augusto M. Agnelli,[2] Jimi Tjong,[1] Mohini Sain[1,3]

[1]Centre for Biocomposites and Biomaterials Processing (CBBP), Faculty of Forestry, University of Toronto, 33 Willcocks Street, Toronto, Ontario M5S 3B3, Canada

[2]Laboratório de Polímeros, Engenharia de Materiais (DEMa), Universidade Federal de São Carlos, Highway Washington Luís (SP-310) Km 235, São Carlos, SP, CEP 13565-905, Brazil

[3]Centre of Advanced Chemistry, King Abdulaziz University, Jeddah 21589, Saudi Arabia

Correspondence to: K. C. Birat (E-mail: b.kc@mail.utoronto.ca)

ABSTRACT: The current work focuses on enhancing the mechanical and thermal properties of sisal fiber reinforced composites that were previously used in developing interior automotive trims. In order to extend their use in other structural applications, two hybrid biocomposites with the combination of sisal (SF) and glass fiber (GF)-SF20/GF10 and SF10/GF20 were blended with polypropylene via extrusion and injection molding process. Critical material properties such as density, fogging, acoustic, mechanical, thermal, and rheological properties were evaluated and results were analyzed using ANOVA. Hybridization of SF and GF enhanced flexural strength and thermal properties of the biocomposites by 33 and 19%, respectively, while no significant change in acoustic, impact and rheological properties were observed. The properties of the hybrid biocomposites were compared with the material specification of a battery tray and it was found that these hybrid biocomposites could be better alternative materials in structural applications. © 2015 Wiley Periodicals, Inc. J. Appl. Polym. Sci. **2015**, *132*, 42452.

KEYWORDS: applications; composites; properties and characterization; thermoplastics; thermal properties

Received 19 March 2015; accepted 4 May 2015

DOI: 10.1002/app.42452

INTRODUCTION

In today's automotive industry, environmental and regulatory requirements are pushing automakers towards the addition of more sustainable and lighter materials in their future products in order to achieve their emission and fuel economy targets.[1] In this scenario, material selection is getting much attention because of its impact in the production process, performance of the parts as well as emissions during service life and end-of-life disposal. Biocomposites are gaining much momentum in the automotive applications as they can offer environmental and economic benefits by light-weighing of the parts and much literature in this area is available to date.[1–4] One of the examples of biocomposites in automotive application is the interior trim parts (30 wt % sisal fiber reinforced polypropylene) developed for Ford model "Ka" is shown in Figure 1. In most cases, commercial use of biocomposites has been limited to nonstructural or semistructural applications due to lower stiffness, impact and thermal properties.[5] Besides, issues of poor rheology and inconsistent supply chain have also been reported.[3,4] In order to consider this existing sisal fiber-based biocomposite for structural application, it is critical to enhance their mechanical and thermal properties while maintaining or improving their processing.

Several studies have shown that hybridization of natural/synthetic fibers can enhance impact, stiffness and thermal properties.[5–8] Nayak and Mohanty[9] hybridized sisal and glass fiber polypropylene to characterize dynamic mechanical and thermal properties. Results showed an enhancement of mechanical properties, increased thermal stability and overall positive hybrid effect at 30% total fiber loading. Severe fiber breakage and loss of properties at fiber loading greater than 30% have previously been reported.[10] Similar results were found by Panthapukkal and Sain[11] on hemp and glass hybrid fiber polypropylene composites. Kalaprasad *et al.*[12] studied melt rheological behavior of sisal and glass fiber hybrid polyethylene as a function of fiber composition, shear stress, shear rate and temperature. This study showed an increase in viscosity and pseudoplastic behavior of the hybrid biocomposite with an addition of fibers. Similarly, Ramesh *et al.*[13] studied mechanical properties of sisal/glass and jute/glass hybrid epoxy composites. Study suggested enhanced tensile properties for sisal/glass and flexural properties

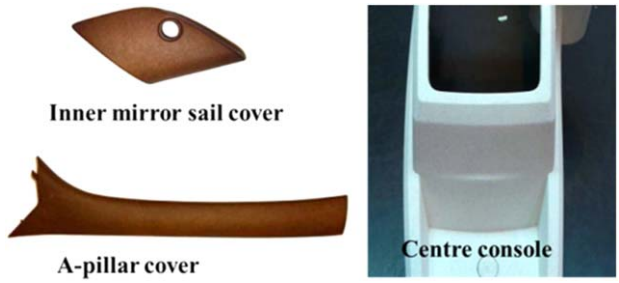

Figure 1. Automotive interior parts made up of 30% sisal fiber polypropylene composite (hSF30/GF0). Courtesy of Ford Motor Company. [Color figure can be viewed in the online issue, which is available at wileyonlinelibrary.com.]

for jute/glass hybrid epoxy composites. Despite numerous reports on hybrid biocomposite characterization, there are few studies that correlate characterization data with the engineering specification of automotive parts.[11,12]

The main objective of this study was to characterize sisal/glass fiber hybrid biocomposite and evaluate its potential for its usage in structural automotive parts, such as engine cover, battery tray, fan shroud, inner door module, and extension panel dash.

Sisal and glass fibers were hybridized with polypropylene. Total volume fraction of fibers was kept at 30% to maintain the rheological properties of currently used biocomposite (30% sisal fiber polypropylene) in Ford 'Ka'. Material properties such as density, fogging, sound absorption, tensile, flexural, impact, heat deflection, and melt viscosity were evaluated. Properties of the hybrid composites were compared with the engineering specification of an automotive battery tray. Additional properties, such as fiber length, scanning electron microscopy (SEM), and thermal analysis were performed to evaluate the effect of glass fiber hybridization in molded part quality and processing temperature requirements.

EXPERIMENTAL

Materials

Two polypropylene grades—impact modified copolymer with MFI 3.5 g/10 min and homopolymer with MFI 40 g/10 min were supplied by Braskem. Sisal fiber (SF) of fiber length 3–5 mm and density 1.1 g/cc was obtained from Hamilton Rios, Brazil and glass fiber (GF) with 10–11 mm length and density 2.5 g/cc was supplied from VI Fiberglass, Brazil.

Composite Fabrication

Sisal fibers were manually mixed with different weight percentage of glass fibers (0, 10, 20 wt %) and polypropylene pellets (Table I). About 3.5 wt % of processing additives, such as coupling agents, processing aids and UV stabilizers were used in each formulation. Samples were dried at 80°C for 4 h in a convection oven and melt-blended in a continuous process using a parallel twin-screw extruder (L/D ratio: 40 : 1, compression ratio: 35%). The extrudates were pelletized using an inline pelletizer and dried for 10 h at 80°C prior to injection molding using 130 ton molding machine (ROMI Pratica 130, Brazil). Injection molding conditions were: injection temperature 195°C, injection pressure: 80 bar, injection time: 9 s and mold temperature: 55°C. In this paper, the term 'hybrid biocomposites' refers to "hSF20/GF10" and "hSF10/GF20".

Characterization

Physical Properties. For density measurement, six samples were cut from ISO tensile specimens and measured using ISO 1183 (Method A) at ambient temperature of 25°C. For theoretical density calculation, rule of mixture was modified for hybrid fibers and void content in the composites was estimated from the difference in experimental and theoretical values.

Sound absorption property of hybrid biocomposites were measured using scanning acoustic microscopy (SAM) at transmission frequency of 1–15 MHz as explained by Baltazar-y-Jimenez *et al.*[15] For determination of fogging characteristics, SAE J1756 standard (photometric method) was used in Labthink FT-F1 fogging tester. Three specimens of 80 ± 2 mm diameter were cut from injection molded rectangular plaques of 120 mm × 160 mm for each hybrid biocomposites and average fogging number was reported after 16 h of conditioning at 100°C.

Morphology of hybrid biocomposite was evaluated using scanning electron microscopy (Inspect S50 SEM). The tensile fractured surfaces were gold sputtered (50 nm) and dried for 30 min in vacuum prior to analysis. For both hybrid biocomposites, fiber length degradation after injection molding process was measured using procedure explained by Panthapulakkal and Sain.[11] Results were compared with theoretically calculated critical fiber length to understand the extent of sisal and glass fiber degradation.

Mechanical Properties. Static tensile and flexural properties were evaluated using a standard mechanical testing machine (Emic DL-3000). Tensile property was measured according to ISO 527 procedure using type 1 specimens at a crosshead speed of 5 mm/min. Flexural property was measured in accordance with ISO 178 procedure in three-point loading model at a crosshead speed of 2 mm/min and span width of 65.6 mm. For Izod impact test, CEAST Resil 25G (hammer velocity 3.46 m/s) was used according to ISO 180 procedure on type 1A specimens. Ten specimens were measured at room temperature for all tests to determine the average value. For heat distortion measurement, CEAST HV6 heat deflection tester was employed using ISO 75-1 method. Three ISO flexural samples for each specimen were cut to 80 mm length and placed in a flatwise position in a heat deflection tester. Temperature at 0.32 mm deflection under 1.80 MPa of applied load was recorded. Dynamic mechanical property was measured on 60 mm × 10 mm × 4 mm specimens

Table I. Formulation of Biocomposite and Hybrid Biocomposite Specimens and their Designation

Designation of samples	PP (wt %)	Sisal fiber (wt %)	Glass fiber (wt %)	Compatibilizer/ additives (wt %)
hPP	96.5	0	0	3.5
hSF30/GF0	66.5	30	0	3.5
hSF20/GF10	66.5	20	10	3.5
hSF10/GF20	66.5	10	20	3.5

Table II. Fiber Length and Density of Injection Molded Biocomposite and Hybrid Biocomposites

Designation of samples	Average fiber length after injection molding process		Experimental density 'ρ_{expt}' (g/cc)	Theoretical density 'ρ_{theo}' (g/cc)	Density difference (%)
	Sisal fiber (mm)	Glass fiber (mm)			
hPP	-	-	0.90 ± 0.01	0.90	−0.13
hSF30/GF0	2.36 ± 0.54	-	1.01 ± 0.01	1.06	5.11
hSF20/GF10	2.14 ± 0.65	0.711 ± 0.13	1.03 ± 0.01	1.17	11.36
hSF10/GF20	2.32 ± 0.71	0.787 ± 0.14	1.11 ± 0.10	1.27	12.95

using dynamic mechanical analyzer (DMA Q800) from TA instruments. Three-point bending force was applied at span of 50 mm using multifrequency controlled strain mode. Samples were exposed to temperature range of −100°C to 150°C at a heating rate of 3°C/min and frequency of 1 Hz.

Thermal Properties. Thermal analysis of hybrid biocomposites was also carried out using thermogravimetric analyzer (TGA Q-50) and differential scanning calorimeter (DSC Q-100) from TA instruments. DSC measurements were calibrated with *Indium* (cell constant = 1.092) and each sample (5–10 mg) was heated from 40 to 220°C at a heating rate of 10°C/min to eliminate thermal history followed by cooling from 220 to 40°C at 10°C/min to detect crystallization behavior and reheated to 220°C to study melting characteristics. For TGA measurements, samples weighing 10–20 mg were heated from 40 to 700°C at a heating rate of 20°C/min. Both studies were performed under nitrogen atmosphere at a flow rate of 50 mL/min.

Melt Viscosity. Rheological property of the hybrid biocomposites was measured using melt flow indexer CSI-127 (Custom Scientific Instruments) as per ISO1133 standard on the extruded pellets. A load of 2.16 kg was applied for melt time of 240 s at 190 and 230°C. An average value from 24 measurements was taken from each sample.

Statistical Analysis

Results were compared using one-way analysis of variance (ANOVA) followed by Tukey's test in statistical software Minitab®14 at 95% confidence interval. Two-way ANOVA was also performed for melt viscosity and sound attenuation data.

RESULTS AND DISCUSSION

Physical Properties

Density. Density of the material is directly related with the automotive part weight and provides design engineers a measure of weight-reduction potential with hybrid biocomposite. The experimental and theoretical densities of hPP, SF, and SF/GF hybrid composites are given in Table II. It was observed that incorporation of sisal fibers and hybrid fibers resulted in an increase in density as compared to hPP. Since glass fiber has higher density than sisal fiber, composite density with higher glass fiber content increased as expected. One-way ANOVA analysis showed density increase by 10% in hSF10/GF20 and no significant difference was found in hSF20/GF10 compared to hSF30/GF0 (R^2 value = 72.3, P value = 0.000). Theoretical densities were calculated using hybrid rule of mixture (Table II). Larger difference between the theoretical values and the experimental results were observed for hybrid biocomposites. From the literature, this can be attributed to poor fiber–matrix adhesion or increased microstructure defects, and higher void frequency.[14–16] These results suggest that hybrid biocomposites will exhibit less than optimal mechanical and thermal performance.

Fogging Properties. Fogging is a measure of volatile constituents of materials at higher service temperature and is a critical material selection parameter for automotive interior applications.[17] One of the major constraints towards the application of biocomposites is higher volatile emissions, odor, and fogging values.[7] Studies have suggested lower volatile organic compounds (VOCs) emission, odor, and fogging via enhanced surface interaction (encapsulation) between natural fibers and thermoset polymers.[17] Results of this study are shown in Figure 2. Compared to hSF30/GF0, only SF10/GF20 showed higher fogging value and can be directly associated with only 10 wt % of sisal fiber content ($P < 0.05$). Reduction of 30 wt % to 20 wt % sisal fiber did not produce significant change in fogging characteristics of SF20/GF10.

Acoustic Properties. Sound absorption is defined a material's ability to reverberate sound.[18] Interior and under-the-hood materials require good sound absorption property in order to minimize noise from engine and transmission. Results of sound absorption are shown in Figure 3. Sound attenuation of all biocomposites increased with the increasing acoustic frequency from 1 to 15 MHz. Based on the two-way ANOVA analysis, comparison of hybrid biocomposites with hSF30/GF0 showed

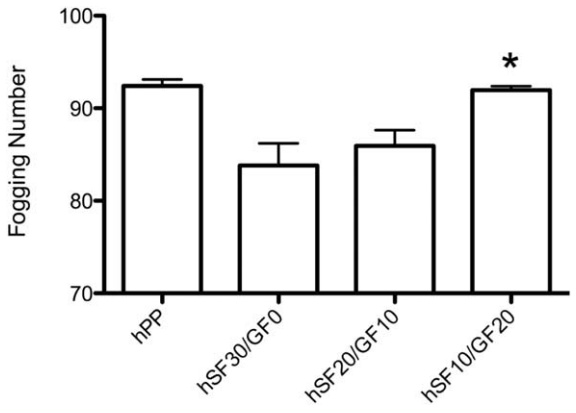

Figure 2. Fogging property of hybrid biocomposites. *$P < 0.05$ hSF10/GF20 compared to hSF30/GF0. Bars represent mean ± 95% SD. One-way ANOVA was used for statistical analysis.

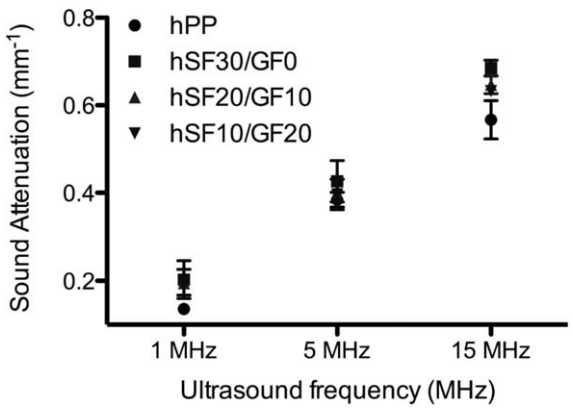

Figure 3. Sound attenuation property at frequency 5, 10, and 15 MHz. No significance was observed between groups. Bars represent mean ± 95% SD. Two-way ANOVA analysis was used for statistical analysis.

that sound absorption value remained constant at all sound frequency tested. Study by Liu *et al.*[19] reported that biocomposites have good sound absorption properties at wide range of frequencies due to porous and fibrous nature of natural fibers. However, the study by Dobircau *et al.*[18] suggested that similar wave propagation phenomenon can be observed with similar wt % of mineral filler or glass fiber. It is possible that equal wt % of fibers in hybrid biocomposites contributed to similar sound absorption pattern.

Fiber Length Analysis. Achieving maximum fiber length of fiber reinforced composites after injection molding process is important for final product performance. Results of fiber length measurement after injection molding process are shown in Table II. Lengths of SF and GF prior to processing were 3–5 mm and 10–11 mm, respectively. Compared to original fiber length, degradation in SF (maximum 53%) was much lower than GF (maximum 93%). This phenomenon directly translates to less than optimal properties of hybrid fiber composites.[18,19] Critical fiber length 'L_c' which is a measure of minimum fiber length required to transfer maximum applied stress from matrix to fiber was estimated for both sisal and glass fiber using Kelly and Tyson model. Calculated 'L_c' for SF and GF were 1.63–2.40 mm and 0.86–2.81 mm, respectively.[20–22] For the calculations, diameter of SF used was 205 μm while GF was 15 μm. From the study, sisal fiber's final length was within the range of 'L_c' while glass fiber's length was slightly below 'L_c'. In other words, stress transferred from matrix to glass fiber was less than its yield strength while sisal fibers were capable of withstanding load to its maximum strength. This result suggests the need for optimization of extrusion and injection molding process.

Mechanical Properties

Tensile and Flexural Properties. Tensile and flexural properties help to predict performance of materials under uniaxial and bending load conditions, respectively. Tensile strength and flexural modulus of hybrid composites are given in Figure 4. Incorporation of 30% SF increased tensile strength of hPP by 63% and modulus by 250%. Tensile strength further increased for two hybrid fiber compositions: hSF20/GF10 and hSF10/GF20 by 86 and 120%, respectively. Flexural modulus further increased by 12% in hSF20/GF10 and 33% in hSF10/GF20 ($P = 0.000$, R^2 value 93.7). Steady increase in tensile strength and flexural modulus with the addition of GF can be attributed to efficient stress transfer as compared to hSF30/GF0. Stress–strain curve of hybrid composites (figure not shown) suggests that hPP showed ductile behavior and strain of failure was greater than 8%, whereas incorporation of sisal and glass fibers rendered brittleness in the matrix and reduced the failure strain to approximately 4%. It is likely due to restriction in polymer motion in the presence of fiber during tensile loading and causing it to fail before reaching its maximum strain to failure. Among the hybrid biocomposites, hSF10/GF20 showed optimum level of stress, which could possibly be due to higher modulus of GF. However, addition of more than 20% of GF in hybrid biocomposites could produce negative hybrid effect as a result of higher fiber agglomeration and fiber–fiber interaction.[11]

Impact Strength. Impact strength reflects the energy required for the propagation of crack via notch or deformation in a material. Figure 5 shows impact energy of notch and un-notched hybrid composites. For un-notched specimens, the impact energy of hPP was significantly reduced upon the addition of 30% fibers. However, introduction of a notch/deformation did not significantly influence impact energy (R^2 value = 0.00, $P = 0.869$). Study by Panthapukkalal and Sain[11] also showed similar result with notched hemp/glass fiber hybrid compositions. In contrast, study by Nayak and Mohanty[9] showed increase in notched impact strength from 57.8 to 63.3 J/m by hybridizing 15% GF with 15% SF. Nonetheless, notched impact values of the composites in our study were significantly higher than biocomposites or hybrid fiber composites reported elsewhere with 30% fiber reinforcement. In hybrid biocomposites, good interfacial strength between fibers and matrix may lead to an increase in impact strength.[9] On the contrary, mixing of two dissimilar fibers usually creates larger voids and nonuniform distribution. Earlier effect leads to a more brittle fracture, whereas the latter leads to easy fiber pull out fracture.[20] As no

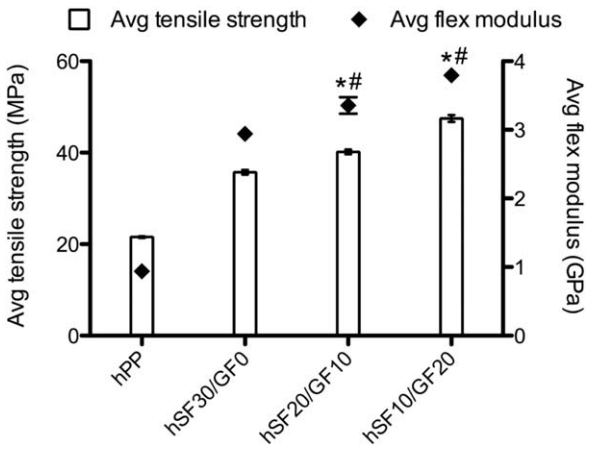

Figure 4. Tensile and flexural properties of hybrid biocomposites. $^{*}P < 0.05$ hSF20/GF10 and hSF10/GF20 compared to hSF30/GF0 for average tensile strength; $^{\#}P < 0.05$ hSF20/GF10 and hSF10/GF20 compared to hSF30/GF0 for average flexural modulus. Bars represent mean ± 95% SD. One-way ANOVA was used for statistical analysis.

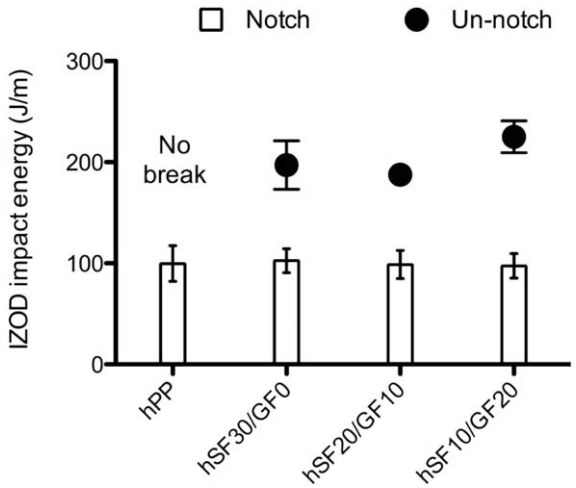

Figure 5. IZOD impact energy of notched and un-notched hybrid biocomposites. Note no break for un-notched hPP. Bars represent mean ± 95% SD. One-way ANOVA analysis was used for statistical analysis.

significant change in notched impact energy was observed in our study, it is possible that the developed hybrid biocomposites experienced balance of both effects.

Surface Morphology. Scanning electron microscopy (SEM) is an important tool to study fiber–matrix interaction and fracture behavior of composites. SEM images of tensile fracture surface at two different magnifications (*a–c* ×100; and *d–f* ×1000) are shown in Figure 6. All hybrid composites exhibited good fiber–matrix interface and fibers were randomly distributed. Few agglomerates of SF were also found in hSF30/GF0 [Figure 6(a)]. Some fiber debonding was observed for transversely oriented SF [Figure 6(a)] and no matrix cracking was found in all composites. Voids varied in sizes from ~30 to 300 μm with more abundance in hSF20/GF10 and hSF10/GF20 [Figure 6(a–c)]. These results are consistent with a higher density difference between experimental data and theoretical values of hybrid fiber composites. Hence, it is possible that despite an increase in tensile, flexural, and heat deflection properties, maximum hybrid effect was not achieved in hybrid fiber composites. In some regions of hybrid fiber composites, glass fibers were pulled out with bulk matrix suggesting inefficient interfacial adhesion [Figure 6(f)]. Overall, fiber breakage and fiber pull-out were the dominant fracture mechanism in hSF30/GF0 and hybrid fiber composites, respectively. Fiber breakage was more common in SF and fiber pull-out for GF [Figure 6(e,f)] This can be explained in terms of GF length that was lower than L_c (see section Fiber Length Analysis) causing fiber pull out fracture in hybrid biocomposites. On the contrary, this might be the case for good impact strength despite higher microstructural defects due to voids and fiber agglomerations as explained in previous sections.

Heat Deflection Temperature (HDT). Heat deflection temperature is a measure of the resistance of a material to deformation

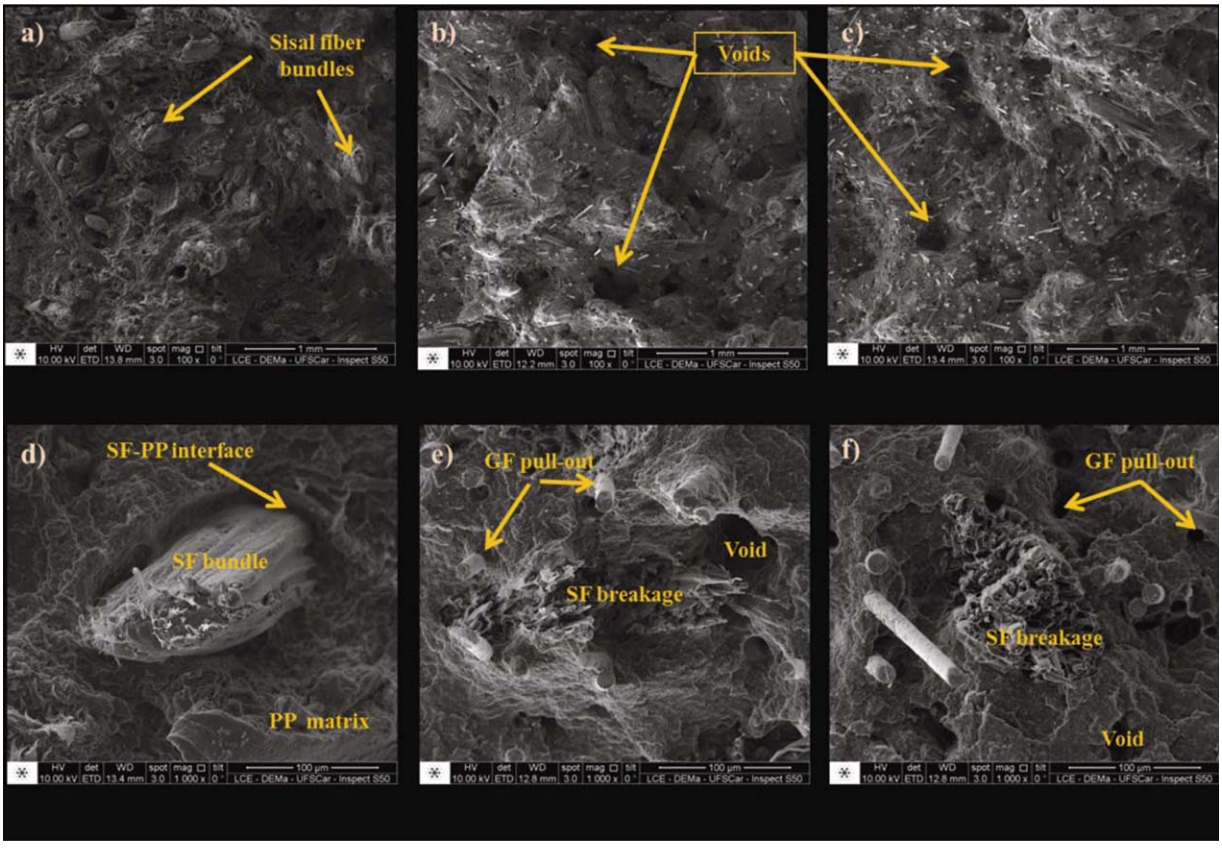

Figure 6. SEM images of hybrid biocomposites. Top and bottom three images represent tensile fracture surface at ×100 (a–c) and ×1000 (d–f) magnifications, respectively. [Color figure can be viewed in the online issue, which is available at wileyonlinelibrary.com.]

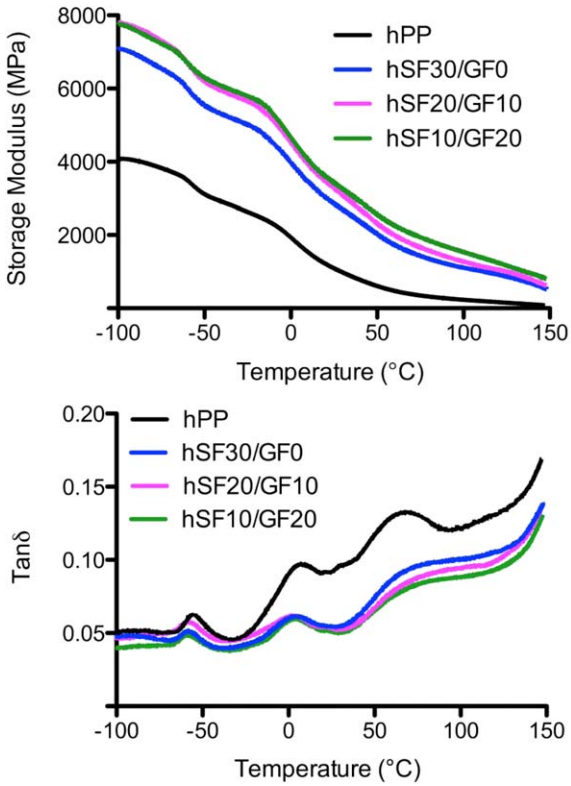

Figure 7. Storage modulus E' (top) and tanδ (bottom) of hybrid biocomposite shPP, hSF30/GF0, hSF20/GF10, and hSF10/GF20 under varying temperature. [Color figure can be viewed in the online issue, which is available at wileyonlinelibrary.com.]

at maximum service temperature and load condition. This is an important property when materials are developed for high temperature and load bearing applications.[11] Addition of SF significantly increased HDT of hPP from 55 to 102°C (R^2 value = 98.03, P value = 0.000). Hybridization of SF and GF further increased HDT by 10% for hSF20/GF10 and 19.3% for hSF10/GF20. This result suggests that hybrid biocomposites have potential to be used in application where maximum service temperature requirement is below 110°C.

Dynamic Mechanical Properties. In order to understand the elastic and viscoelastic behavior of hybrid biocomposites over a wide temperature range, dynamic mechanical analysis (DMA) was performed. Figure 7 shows storage modulus, which is an ability of hybrid fibers (elastic component) to retain the stored energy from −100°C to 150°C. Maximum storage modulus was found for hSF10/GF20 followed by hSF20/GF10, hSF30/GF0, and hPP, which is consistent with flexural modulus values as shown in Figure 4. At −40°C, storage modulus increased from approximately 5 to 6 GPa with hybridization. For hybrid biocomposites, despite a decline in modulus with an increase in temperature, the decrease was not catastrophic and retained approximately 50% of the stiffness at 100°C. A lower tan δ (damping factor) value was found for hybrid biocomposites, which could be due to a restriction in polymer motion as a result of fiber incorporation (Figure 7). These results infer that hybridization of SF and GF can improve the thermal stability over wide range of temperature.

Thermal Properties

Melting and crystallization behavior of hybrid biocomposites were measured using DSC (Table III). Results showed that addition of sisal and glass fiber did not significantly influence melting and crystallization temperature. However, it interrupted linear melting as well as crystallization behavior of hPP and significantly lowered the enthalpy. Study by Zhang *et al.*[16] found reduced enthalpy of PP with the addition of wood flour and short glass fibers . Similar trend was found for maximum degree of crystallinity (X_c) of hybrid fiber composites calculated using eq. (1).

$$X_c = \frac{\Delta H_m}{V_m \Delta H_m^*} \times 100 \quad (1)$$

where $\Delta H_m, V_m$, and ΔH^* are enthalpy of melting of composition, volume fraction of polypropylene blend and enthalpy of 100% crystalline polypropylene, respectively. ΔH^* value used in the calculation was 209 J/g.[23] Results of DSC are summarized in Table 4. Nayak *et al.*[24] found an increase in X_c with the incorporation of hybrid fibers due to formation of nucleation sites. However, addition of maleated PP (MAPP) hindered the linear crystallization behavior of PP matrix resulting in lower X_c values. It is possible that addition of MAPP in all biocomposites formulation decreased the crystallinity of hPP matrix and enhanced the interfacial adhesion between fiber and matrix shown by SEM results. In comparison to hSF30/GF0, hybrid biocomposites showed a slight increase in X_c. This could be due to an increase in nucleation site from a relatively small diameter (10 μm) of glass fibers.

Thermal stability of hybrid biocomposites was also investigated by TGA. Results suggest that the incorporation of glass fiber reduced the rate of decomposition and enhanced the thermal stability (Figure 8). First derivative of TGA thermograms plotted against temperature (figure not shown) showed second peak at

Table III. Comparative DSC Results for Biocomposite and Hybrid Biocomposites

Designation of samples	Melting temperature (°C)	Enthalpy melting, ΔH_m (J/g)	Crystallization temperature (°C)	Enthalpy crystallization, ΔH_f (J/g)	Degree of crystallinity (X_c)
hPP	164.18	73.92	118.9	81.22	35.4
hSF30/GF0	164.31	34.9	118.03	49.05	24.9
hSF20/GF10	164.61	41.1	117.52	53.56	29.0
hSF10/GF20	164.63	39.25	117.97	50.41	27.7

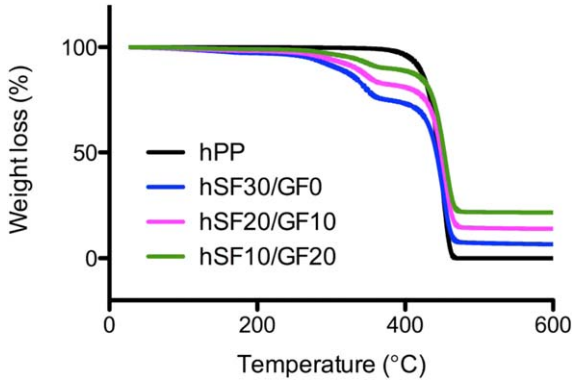

Figure 8. TGA thermograms of hybrid biocomposite shPP, hSF30/GF0, hSF20/GF10, and hSF10/GF20. [Color figure can be viewed in the online issue, which is available at wileyonlinelibrary.com.]

190–375°C which could be associated with decomposition of cellulose and hemicellulose.[25] Initiation of decomposition (2nd peak) started at 190, 210, and 230°C for hSF30/GF0, hSF20/GF10, and hSF10/GF20, respectively. Compared to SF30/GF0, incorporation of sisal/glass hybrid fibers increased the initiation of hPP decomposition (3rd peak) from 340 to 380°C which is consistent with the TGA results by Zhang *et al.*[26] This result suggests that wider range of processing temperatures is possible for hybrid biocomposites.

Melt Viscosity

Melt flow rate (MFR) of composite is one of the important criteria for selecting materials in injection molding application.[24] It measures the viscosity change with the temperature and is indicative of the suitability for processing.[6] Figure 9 shows the melt flow measurement of hybrid biocomposites at 190 and 230°C. Results at 190°C showed that an addition of 30% SF reduced flow of hPP by 65%. Similar results have previously been reported where an addition of fibers increased the surface

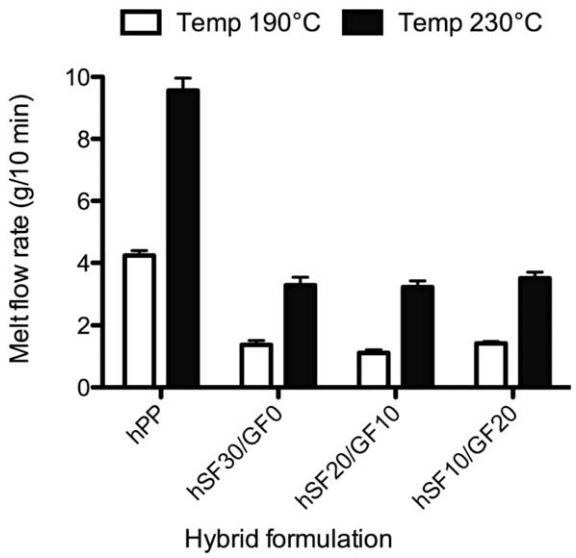

Figure 9. Melt flow rate of hybrid biocomposites at 190 and 230°C. No significance was observed between groups. Bars represent mean ± 95% SD. Two-way ANOVA analysis was used for statistical analysis.

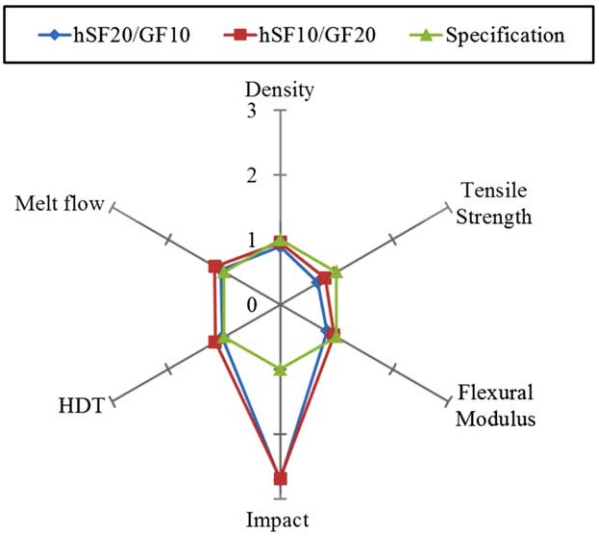

Figure 10. Relative properties of hybrid biocomposites compared with specification of battery tray cover (data not shown due to confidential agreement with Ford Motor Company). [Color figure can be viewed in the online issue, which is available at wileyonlinelibrary.com.]

area and thus, hindered the flowability of polypropylene molecules.[27] Linear increase was found for all composites with the increase of melt temperature from 190 to 230°C. Comparison of hSF30/GF0 with hybrid biocomposites did not have a significant change in the melt viscosity, which suggests that similar injection pressure and holding pressure could be used.

Comparison with the Current Automotive Structural Specification

In order to demonstrate the functional capability of the developed hybrid biocomposite, a comparison was made with the specification of an automotive battery tray (Figure 10). According to the specification, battery tray must withstand heat and vibration from engine exhaust pipes and engine, impact from falling objects during service requirements and more importantly, must be resistant to engine fluids, such as engine oil, coolant, washer fluid, sulfuric acid.[28] Additional requirements include flammability, melt flow (quick measure of clamp tonnage requirement), and heat aging performance. The current comparison showed both hybrid biocomposites' HDT, melt flow, and flexural modulus were similar while both exceeded impact requirements. Furthermore, the density of hybrid fiber composites was slightly lower compared to currently used material in battery tray suggesting an opportunity for up to 10% weight reduction. This comparison indicates that developed hybrid fiber composites have a potential to be used in developing a battery tray prototype. Based on dynamic and static mechanical test, hybrid biocomposites showed superior performance to SF30/GF0 and are expected to meet the heat aging performance criteria. Additional tests, such as flammability and chemical resistance need to be evaluated and will be the future objectives of this research.

Other potential under-the-hood application of developed hybrid biocomposite include air induction integrated parts and extension panel dash that have similar specification to battery tray. Due to

significantly higher impact resistance, hybrid biocomposites can be used to develop under-body shield, belly pan and wheel liner. Fogging test and sound absorption test also showed no significant change in hybrid biocomposites compared to hSF30/GF0 suggesting that they can also be considered for interior application such as inner door module and extension panel dash.

CONCLUSIONS

Overall, this paper has demonstrated that the sisal/glass fiber hybrid biocomposites have a balance between strength, impact, heat deflection, and flow properties required for automotive structural applications. Both hybrid fiber composites; hSF10/GF20 and hSF20/GF10 exhibited positive hybrid effect during static tensile and flexural tests, higher storage modulus, lower tanδ peaks and better thermal stability compared to hSF30/GF0. Comparison of hybrid biocomposites with the current battery tray specification showed that both met critical performance criteria such as stiffness, HDT, and impact resistance and have a potential to be used in a prototype development. Due to significantly higher impact properties, hybrid biocomposites can be used in high impact applications such as wheel liners. Similar sound absorption and fogging behavior to the reference material SF30/GF0 also suggest their use in structural interior parts such as inner door module. Based on the thermal data, melting and crystallization temperature of hybrid biocomposites remained similar but the initiation of degradation temperature increased up to 230°C. SEM results showed good fiber–matrix interface and fiber dispersion. However, fiber length analysis showed severe fiber breakage suggesting the need for optimizing injection molding process parameters prior to high-volume production. Overall, developed hybrid biocomposites have increased mechanical and thermal properties without compromising impact and melt viscosity and thus, their application could be extended to automotive structural parts in the future.

ACKNOWLEDGMENTS

The authors would like to thank CAPES-DFAIT program and Automotive Partnership Canada (APCJ 433821-12) for funding this research. We are also thankful to all the technical staffs at DEMa, UFSCAr (Brazil) and Ford Powertrain Engineering Research and Development Centre (Windsor, ON) for providing support to this research project.

REFERENCES

1. Vaidyanathan, H. P; Murty, P.; Eswara, S. P. *SAE Int.* **2011**, *01*, 0219.
2. Sathaye, A. *SAE Int.* **2011**, *01*, 0224.
3. Sopher, S. R.; Sasaki, H. *SAE Int.* **2012**, *01*, 0942.
4. Ademuwagun, A.; Myers, J. *SAE Int.* **2014**, *01*, 1026.
5. Maleque, M. A.; Atiqah, A.; Iqbal, M. *Adv. Mater. Res.* **2012**, *576*, 471.
6. Youssef Ramzy, A.; El-Sabbagh, M. M. A.; Steuernagel, L.; Ziegmann, G.; Meiners, D. J. *Appl. Polym. Sci.* **2014**, *131*, 3.
7. Summerscales, J.; Dissanayake, N.; Virk, A.; Hall, W. *Compos. A Appl. Sci. Manuf.* **2010**, *41*, 10.
8. Panthapulakkal, S.; Sain, M. *J. Compos. Mater.* **2007**, *41*, 15.
9. Nayak, S. K.; Mohanty, S. *J. Reinforced Plast. Compos.* **2009**, *29*, 10.
10. Himani, J.; Purnima, J. *Mater. Sci. Eng. A* **2010**, *527*, 7.
11. Panthapulakkal, S.; Sain, M. *J. Appl. Polym. Sci.* **2007**, *103*, 2032.
12. Kalaprasad, G.; Mathew, G.; Pavithran, C.; Thomas, S. *J. Appl. Polym. Sci.* **2003**, *89*, 432.
13. Ramesh, M.; Palanikumar, K.; Reddy, K. H. *Proc. Eng.* **2012**, *51*, 745.
14. Qatu, M. S. *SAE Int.* **2011**, *01*, 0215.
15. Baltazar-y-Jimenez, A.; Seviaryna, I.; Sain, M.; Maeva, E. Y. *J. Reinforced Plast. Compos.* **2011**, *30*, 16.
16. Faruk, O.; Bledzki, A. K.; Fink, H.-P.; Sain, M. *Prog. Polym. Sci.* **2012**, *37*, 11.
17. Bendo, A.; Nordmann, G.; Norton, J.; Funk, J.; Kalbe, M.; Reck, B.; Gerst, M.; Corp, B. *SAE Int.* **2011**. DOI: 10.4271/2011-01-0220.
18. Dobircau, L.; Rupert, L.; Turner, J.; Delbreilh, L.; Dargent, E.; Saiter, J. M. *Macromol. Symp.* **2013**, *28*, 1.
19. Liu, D.; Xia, K.; Yang, R.; Li, J.; Chen, K.; Nazhad, M. *J. Compos. Mater.* **2012**, *46*. 9.
20. Sain, M.; Panthapulakkal, S.; Law, S.; Bouillous, A. *J. Reinforce. Plast. Compos.* **2005**, *24*, 2.
21. Peltola, H.; Madsen, B.; Joffe, R.; Nättinen, K. *Adv. Mater. Sci. Eng.* **2011**, *2011*, 1.
22. Idicula, M.; Malhotra, S. K.; Joseph, K.; Thomas, S. *Compos. Sci. Technol.* **2005**, *65*, 7.
23. Rahman, W. A. W. A.; Isa, N. M.; Rahmat, A. R.; Adenan, N.; Ali, R. R. *Adv. Mater. Res.* **2009**, *83*, 367.
24. Nayak, S. K.; Mohanty, S.; Samal, S. K. *Mater. Sci. Eng. A* **2009**, *523*, 1.
25. Sun, Z. Y.; Han, H. S.; Dai, G. C. *J. Reinforce. Plast. Compos.* **2009**, *29*, 5.
26. Zhang, X.; Yang, H.; Lin, Z.; Tan, S. *J. Thermoplast. Compos. Mater.* **2011**, *26*, 01.
27. Nurul, M. S.; Mariatti, M. *Polym. Bull.* **2012**, *70*, 03.
28. Material and Toxicology System (MATS) Online Library: WSS-M15P50-B. Accessed May, **2014**.